Journal of Green Energy Research and Innovation

Optimal Novel Fuzzy Control Design Method for Efficient Grid-Connected Photovoltaic System

Asaad Shemshadi, Hamidreza Haghighi

Highlights

- **A three-input fuzzy logic controller (E, CE, Vpv) is proposed for improved MPPT in grid-connected PV systems.**
- **PSO optimization enhances fuzzy membership functions, reducing oscillations and improving accuracy.**
- **The method outperforms the P&O algorithm under varying irradiance and temperature.**
- **Hysteresis current and PID control ensure stable grid synchronization and power injection.**
- **MATLAB simulations show reduced ripple and higher energy transfer efficiency.**

Graphical Abstract

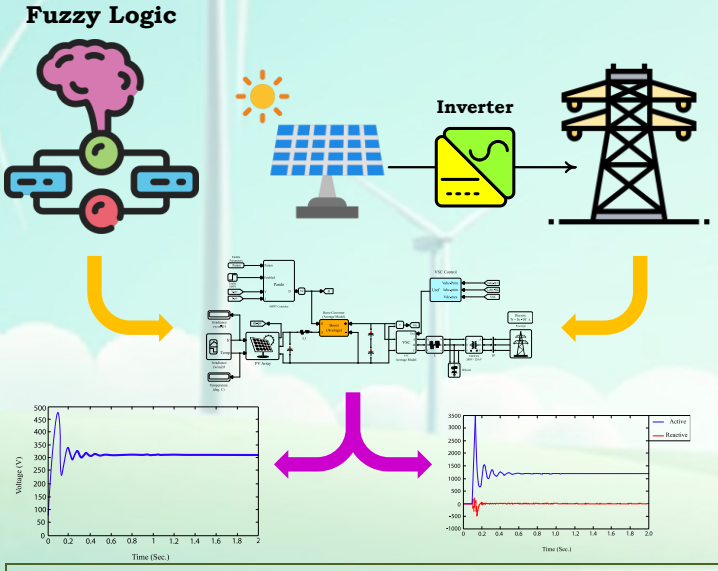

Use your device to scan and read the article online

Citation

A. Shemshadi and H. Haghighi," Optimal Novel Fuzzy Control Design Method for Efficient Grid-Connected Photovoltaic System," *Journal of Green Energy Research and Innovation*, vol. 2, no. 3, pp. 27-43, 2025.

https://doi.org/10.61882/jgeri.2.3.27

Journal of Green Energy Research and Innovation 2.3 (2025) 27-43

Online ISSN: 3041-9018

Journal of Green Energy Research and Innovation

Journal Homepage: www.jgeri.araku.ac.ir

Optimal Novel Fuzzy Control Design Method for Efficient Grid-Connected Photovoltaic System

Asaad Shemshadi * , Hamidreza Haghighi

Department of Electrical Engineering, Arak University of Technology, Arak, Iran.

A R T I C L E I N F O

Keywords:
fuzzy logic controller, power point tracking, inverter, particle swarm algorithm.

Article History:
Received: 02 March 2025;
Revised: 06 May 2025;
Accepted: 12 May 2025.

Article type:
Research Article

* ***Corresponding author***
E-mail address
shemshadi@arakut.ac.ir (A. Shemshadi)

A B S T R A C T

In this article, the modified fuzzy controller tracks the maximum power point (MPP) in a photovoltaic (PV) system connected to the grid under variable and standard solar radiation and variable temperature conditions. The perturb and observe (P&O) method has also been employed for MPP tracking (MPPT), and it has been compared with the modified fuzzy method. Ultimately, the superiority of the modified fuzzy method has been proven. In addition, the particle swarm algorithm (PSO) is employed to make the fuzzy groups optimal, thereby enhancing the performance of the fuzzy controller. In conclusion, implementing the designed phase control for the PV system connected to the single-phase grid is paramount. Furthermore, utilizing the hysteresis current control method facilitates inverter switching, thereby ensuring the injection of maximum power into the grid.

1. Introduction

The grid-connected PV system comprises a PV module, a boost converter, and a maximum power point tracking (MPPT) system, which together enable integration with the main power grid. In this method, the electrical energy generated by the PV system is integrated into the main grid through grid-connected inverters, which modify the waveform and adjust key parameters such as voltage level, phase angle, and frequency to ensure compatibility [1-4].

1.1. Research Necessity and Novelty

The growing global energy demand and environmental concerns have led to the increased integration of PV systems into modern power grids. However, variations in solar radiation and temperature cause continuous fluctuations in PV output, reducing system reliability and energy utilization. An intelligent and adaptive MPPT method is essential to maintain optimal operation and guarantee efficient grid interaction. The necessity of this study arises from the need for an improved control strategy capable of minimizing power ripple, improving transient response, and ensuring seamless grid synchronization. The key novelty of this work lies in proposing a modified fuzzy logic controller optimized using the PSO algorithm. Unlike conventional two-input fuzzy controllers, the proposed method introduces a third input (PV voltage) to enhance decision precision. PSO is used to optimally adjust the membership function parameters—centers and spreads—thereby reducing power fluctuations and improving MPPT accuracy. Moreover, the proposed controller is integrated into a grid-connected PV configuration, where hysteresis current control and a PID-based synchronization system ensure efficient power injection into the grid [5-9].

1.2. Contributions

The main contributions of this study are summarized as follows:

1. Development of an enhanced fuzzy MPPT controller with three inputs (E, CE, and V_{pv}) for improved tracking performance.
2. Optimization of fuzzy membership functions using PSO, leading to reduced oscillations and enhanced steady-state accuracy.
3. Implementation of the proposed control method in a grid-connected PV system with effective hysteresis-based current synchronization.
4. Comparative analysis demonstrating superior efficiency and stability compared to the conventional P&O algorithm under dynamic conditions.

1.3. Paper Organization

The remainder of this paper is organized as follows. Section 2 provides a general overview of solar energy and power systems, discussing the role of PV technologies in sustainable energy generation and the challenges of their integration into modern grids. Section 3 describes the modeling of MPPT in PV systems, including equivalent electrical circuit representation, operational characteristics, and the governing current–voltage relationships under variable irradiance and temperature conditions. Section 4 presents the proposed optimal fuzzy controller design for MPPT, explaining its structural framework, control mechanism, and advantages over conventional methods. Section 5 outlines the Particle Swarm Optimization (PSO) algorithm used to fine-tune the fuzzy controller's parameters, detailing its mathematical formulation, optimization strategy, and convergence process. Section 6 elaborates on the fuzzy logic controller design and optimization procedure, covering the fuzzification, rule inference, and defuzzification stages, as well as the incorporation of PSO-based parameter adjustment. Section 7 reports the MATLAB-based simulation results, providing a comparative performance analysis between the proposed optimized fuzzy control method and the conventional Perturb and Observe (P&O) algorithm for both standalone and grid-connected PV systems. Finally, Section 8 concludes the paper by summarizing the key findings, verifying the effectiveness of the proposed control strategy, and suggesting possible directions for future research.

2. Solar Energy and Power Systems

Currently, large-scale PV systems, configured as renewable power substations, are integrated into the power grid through power electronic converters, as illustrated in Figure 1.

Figure 2 illustrates that the equivalent circuit of a PV cell incorporates both series and parallel resistances. The series resistance represents the cumulative resistive effects of the semiconductor material and electrical interconnections, and its value increases with the number of cells connected in series. The parallel, or shunt, resistance models power losses due to small leakage currents through alternate conduction paths. While series resistance can significantly influence performance, the impact of parallel resistance is generally minimal. Additionally, the behavior of non-ohmic currents in the depletion region can be represented by introducing a second diode into the equivalent circuit model.

Considering all parameters, the current equation of the PV cell will be as described in Equation (1):

$$I = I_{ph} - I_o * (e^{q*(V+I*Rs)/(n*k*T)} - 1) - (V + I * R_S/R_{Sh}) \quad (1)$$

To calculate the value of R_S, we will have Equation (2):

$$R_S = -\frac{dI}{dv} - \frac{n*k*\frac{T}{q}}{Io*e^{\left(q*\frac{V+I*Rs}{n*k*T}\right)}} \quad (2)$$

The value $(\frac{dI}{dv})$ will be determined using the voltage-current characteristic of the PV module.

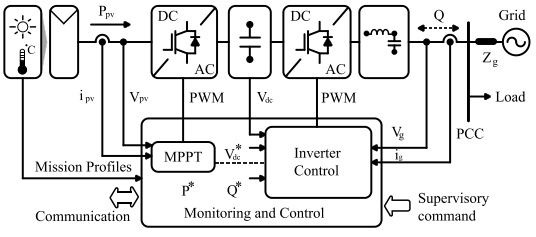

Figure 1. Overview of the PV system connected to the power grid.

3. MPPT in PV systems

Over the past decade, significant attention has been directed toward enhancing the efficiency of PV systems, with MPPT emerging as a key area of focus. MPPT techniques are designed to optimize the extraction of electrical power from PV modules by continuously adjusting the operating point to correspond with the maximum power output. Typically implemented through electronic power converters, these systems actively respond to variations in environmental factors such as solar irradiance and temperature, as well as changes in electrical load, to maintain optimal energy conversion performance.

MPPT is a key factor in improving the energy conversion efficiency of PV systems, thereby enhancing their economic viability. The current–voltage (I–V) curve of PV modules exhibit strong nonlinearity and are affected by several dynamic parameters, such as cell temperature, incident solar radiation, charge carrier lifetime, and the electrical load profile. For any given set of environmental conditions—specifically, irradiance and temperature—there exists a unique operating point on the I–V curve where the module achieves its peak power output. A plethora of methods have been introduced for MPP detection, and they can be classified into four main methodological categories based on their underlying principles [10-12].

The first category includes techniques based on basic algorithmic approaches, with P&O and Incremental Conductance (INC) being the most widely used. The P&O technique functions by slightly adjusting the terminal voltage and observing the corresponding change in output power. If power output rises, the adjustment continues in the same direction; if it falls, the direction of perturbation is reversed. One of the main strengths of this method is its independence from the specific parameters of the PV module [13,14].

However, its primary drawback is the tendency to oscillate around the MPP, especially under rapidly fluctuating environmental conditions, which may result in diminished tracking accuracy.

The second category comprises methods grounded in solar cell modeling. These techniques entail the development of a mathematical or electrical model of the solar cell and the subsequent derivation of its characteristic relationships. The model is then used to predict the behavior of the PV module, thereby serving as the basis for system design and implementation. While such approaches can offer high precision under controlled conditions, their primary limitation lies in their lack of adaptability. Specifically, these methods are customized to the characteristics of a particular solar cell, making it difficult to substitute or upgrade components without requiring a complete redesign of the system [15-18].

The third category comprises techniques that utilize the empirical relationship between the operating point and specific parameters of the PV cell. Notable examples include the short-circuit current method and the open-circuit voltage method. These approaches estimate the MPP based on proportionality assumptions, such as a fixed ratio between the MPP current and the short-circuit current, or between the MPP voltage and the open-circuit voltage. However, their accuracy is limited due to the inherent nonlinearity of the current–voltage characteristics, which undermines the validity of the linear approximations on which these methods rely. The fourth category is intelligent control designs, in which fuzzy logic control or artificial neural networks are used. The fuzzy logic control method can work with imprecise and non-linear inputs and does not require a precise mathematical model. Fuzzy control has three stages: fuzzification, determining rules based on lookup tables, and defuzzification [19,20].

In the fuzzification process, numerical input variables are turned into linguistic variables using predefined membership functions. For fuzzy controllers applied in MPPT, the typical inputs are the error (E) and the change in error (ΔE or CE). The calculation of E and CE can be defined by the system designer, offering flexibility in controller design as in Equations (3) to (4).

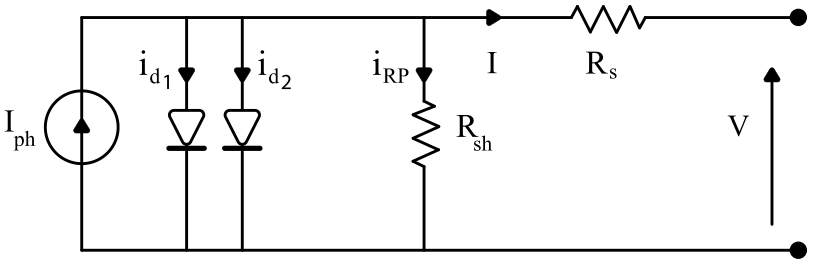

Figure 2. The exact equivalent circuit of the PV cell.

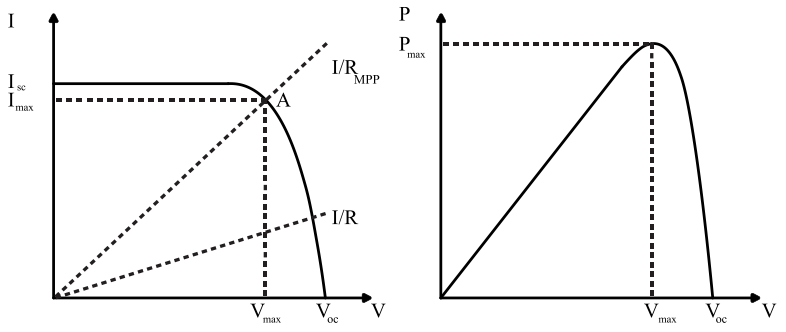

Figure 3. The point of maximum power in the nonlinear PV characteristic.

One common approach involves using the condition where the derivative of power with respect to voltage (dP/dV) approaches zero, which indicates the operating point corresponding to the maximum power.

$$E(n) = \frac{p(n)-p(n-1)}{V(n)-V(n-1)} \quad (3)$$

$$CE(n) = E(n) - E(n-1) \quad (4)$$

CE and E are calculated and converted into linguistic variables. The output of the controller is usually the change in duty cycle of the converter (ΔD) and is searched in the rules table. In the defuzzification step, the output of the fuzzy controller is converted from linguistic variables to numerical variables that are still used in the membership function.

These controllers demonstrate effective performance under varying weather conditions. Experimental results indicate that they achieve rapid convergence to the MPP while exhibiting minimal oscillations around it. The accuracy and stability of the tracking process are significantly influenced by the selection of the membership function, which plays a critical role in shaping the controller's responsiveness and precision.

Each method of finding MPPT has its advantages and disadvantages. In this article, since the goal of optimization is achieved, the maximum efficiency of the PV system, the fuzzy method is used with corrections to reach the maximum efficiency, and the simulation results It is compared with the common P&O method.

4. Optimal Fuzzy Controller Design for MPPT

The MPP of a PV module varies in response to changing environmental conditions, such as irradiance and temperature. Consequently, achieving maximum power transfer would ideally require continuous adjustment of the load, which is not feasible in practical applications. To address this limitation, an intermediate stage is introduced to ensure optimal power extraction from the PV module under constant load conditions and varying environmental inputs. This stage typically involves a DC–DC converter, which may be configured as a step-up, step-down, or bidirectional (buck–boost) converter, depending on the system design requirements. When interfacing with an AC load or the utility grid, a DC–AC inverter must be added following the DC–DC converter [21-24]. This inverter may employ pulse-width modulation (PWM) to boost efficiency and lead to low harmonic distortion, or a simpler square-wave design that offers easier control at the expense of increased harmonic content.

4.1. Boost converter

The converter's placement between the PV module and the consumer is pivotal for effective power extraction. When utilized in conjunction with appropriate control mechanisms, this configuration enables the PV module to operate at its optimal power output level. The boost converter is a device that functions to amplify the direct current (DC) voltage. It is a component of various peak power tracking methods. Given that the maximum voltage produced by the array is negligible, this converter can be utilized to augment the voltage. The ideal model of a boost converter is as follows:

The circuit's operation can be described in two distinct modes. In the first mode, initiated at time $t = t_0 = 0$, the switch is closed, causing the input voltage to be applied across the inductor. As a result, an increasing current flow through the inductor LL and the closed switch. The second mode begins at $t = D \cdot T$, where DD is the duty cycle and TT represents the switching period. At this point, the switch opens, redirecting the inductor current through the diode, capacitor, and load. During this interval, the inductor releases its stored energy to the load, causing the current to gradually decrease. In the subsequent cycle, when the switch closes again, the inductor begins a new energy storage phase. This cyclical operation enables controlled energy transfer to the load (Figure 5).

As illustrated in Figure 6, the status when the switch is closed is as follows in Equations (5) to (7):

$$I_{c1}(t) = C_1 \frac{dv_1(t)}{dt} = i(t) - i_l(t) \quad (5)$$

$$I_{c2}(t) = C_2 \frac{dv_o(t)}{dt} = -i_o(t) \quad (6)$$

$$V_1(t) = L \frac{di_l(t)}{dt} = v_i(t) \quad (7)$$

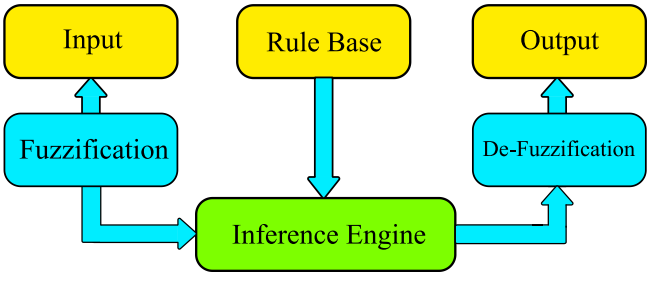

Figure 4. Fuzzy system overview.

As illustrated in Figure 7, the status when the switch is closed is as follows in Equations (8) to (10):

$$I_{c1}(t) = C_1 \frac{dv_1(t)}{dt} = i(t) - i_l(t) \tag{8}$$

$$I_{c2}(t) = C_2 \frac{dv_o(t)}{dt} = i_l(t) - i_o(t) \tag{9}$$

$$V_l(t) = L \frac{di_l(t)}{dt} = v_i(t) - v_o(t) \tag{10}$$

Therefore, it can be concluded that the inductor voltage waveform is illustrated in Figure 8. Voltage and current waveforms for the case where the load current is continuous are as mentioned in Figures 9 to 11.

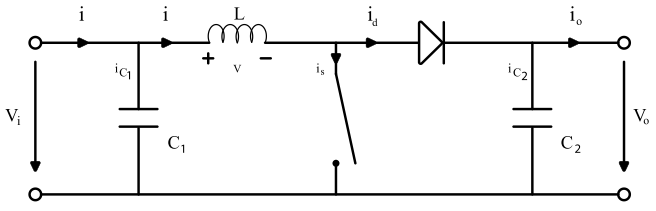

Figure 5. Equivalent circuit of ideal boost converter.

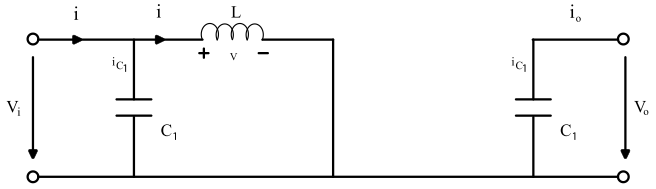

Figure 6. Boost converter in switch closed mode.

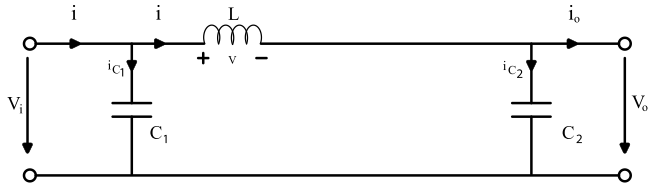

Figure 7. Boost converter in open mode.

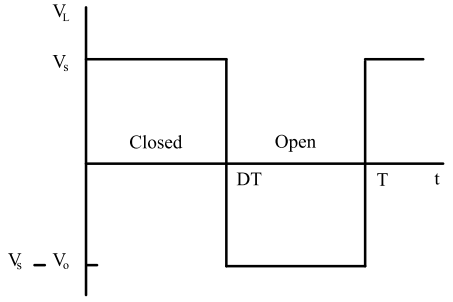

Figure 8. Inductor voltage.

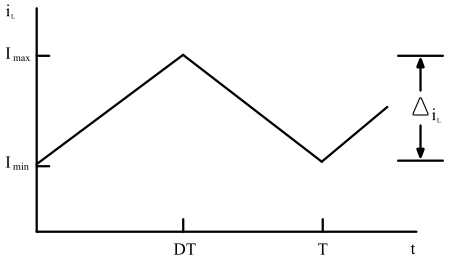

Figure 9. Inductor current.

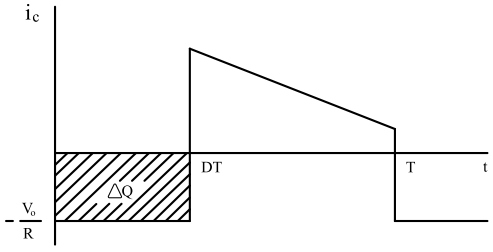

Figure 10. diode current.

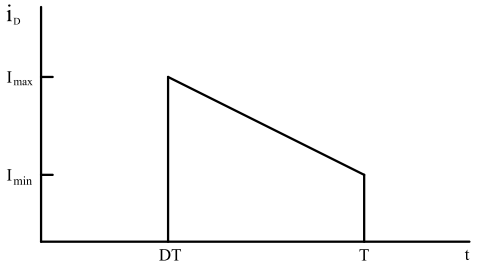

Figure 11. Capacitor current.

The following relations can be obtained for the DC-DC step-up converter (Equation (11) and Equation (12)):

$$V_O = \frac{VS}{1-D} \tag{11}$$

Boost factor:

$$\frac{Vo}{Vin} = \frac{Iin}{Io} = \frac{1}{1-D} \tag{12}$$

4.2. Boost converter design

To have a continuous current flow, the minimum inductance value would be calculated as follows in Equation (13):

$$L_{min} = \frac{(1-D)^2 DR}{2F} \tag{13}$$

In Equation (13), D is the working parameter, R is the consumer resistance in ohms, and F is the switching frequency in Hz. The output capacitor in the boost converter supplies the output current to the consumer when the diode is off. The minimum capacity of the capacitor in this converter is obtained by considering the voltage fluctuation from the Equation (14):

$$C_{min} = \frac{D \times Vo}{2RF} \tag{14}$$

In Equation (14), V_O is the output voltage of the converter.

4.3. Inverter

Solar panels inherently produce direct current, which must be converted to alternating current (AC) for grid connection or AC load applications. This conversion is accomplished using an inverter. A typical single-phase bridge inverter consists of four power electronic switches arranged to alternate the direction of current flow, thereby generating an AC output from a DC input. The type of switching devices, commonly insulated gate bipolar transistors (IGBTs) or metal-oxide-semiconductor field-effect transistors (MOSFETs), is selected based on design requirements. IGBTs are generally preferred for high-frequency switching, while MOSFETs are suitable for applications involving lower frequencies and higher power levels. Various switching control strategies are employed to regulate inverter operation, including conventional pulse width modulation (PWM), sinusoidal PWM (SPWM), and square-wave control with adjustable pulse widths. Each method presents trade-offs in terms of harmonic content, efficiency, and implementation complexity, and the choice depends on the specific performance goals of the inverter system.

The circuit model of a single-phase inverter is illustrated in Figure 12. As shown, the inverter comprises four power switches arranged in a bridge configuration, which facilitate the conversion of DC input to AC output by appropriately controlling the conduction of each switch. To protect the switches during load commutation, especially in the presence of inductive (self-reactive) loads, a freewheeling diode is connected in parallel with each switch. These diodes provide an alternative current path during switch-off intervals, preventing voltage spikes and minimizing the risk of damage to the switching devices.

The inverter has two modes of operation. In the first case, the work cycle interval D, when the switches S1 and S2 are closed, and in the second case, the complementary time 1-D, when the switches S3 and S4 are closed (Figure 13).

5. Particle Swarm Optimization

To enhance the performance of the fuzzy logic controller, the particle swam optimization (PSO) algorithm is employed to optimize the membership functions. PSO is a population-based metaheuristic inspired by the principles of collective intelligence and social behavior, particularly as observed in flocking birds or schooling fish. In this approach, each potential solution—referred to as a 'particle'—navigates the search space with an associated fitness value, which is determined based on its position relative to the objective function. Each particle retains knowledge of its personal best position (Pbest), the best position found by its neighbors (Nbest), and the best position discovered globally by the swarm (Gbest). When the neighborhood includes the entire swarm, Nbest and Gbest are identical. Particles adjust their velocities and positions by considering both their individual experiences and those of their peers. This iterative process allows the swarm to converge toward an optimal or near-optimal solution. By leveraging this algorithm, the fuzzy system can dynamically refine its rule base or membership functions, thereby improving overall tracking accuracy and controller performance. The particle mass optimization algorithm is as follows:

- N particles are created randomly.
- For all particles, speed and position are generated randomly.
- As long as the completion conditions are not met:
  - One unit is added to t.
  - Calculates the value of the objective function for each particle.
  - For i from one to n:

- Calculates $X^{i,best}[t]$
- Next value i is entered.
- Calculates $X^{g,best}[t]$.
- For i from one to n:
  - for j from one to d:

$$V_j^i[t+1] = WV_j^i[t] + c_1r_1(X_j^{i,best}[t] - X_j^i[t]) + c_2r_2(X_j^{g,best}[t] - X_j^i[t])$$
$$X_j^i[t+1] = Xji[t] + V_j^i[t+1]$$

  - Next value j is entered.
- The next value i is entered.

6. Fuzzy Logic controller design and optimization

Given the inherently variable nature of solar irradiance, the MPP of a PV module shifts dynamically along different current–voltage (I–V) curves. Therefore, the MPPT controller must respond rapidly and accurately to these changes to minimize power fluctuations and reduce energy losses. Among the various MPPT strategies, intelligent control techniques—particularly fuzzy logic-based methods—have gained prominence in recent years, often outperforming conventional approaches such as P&O and INC. Due to their heuristic nature, robustness, and effectiveness in both linear and nonlinear systems, fuzzy controllers are well-suited for real-time MPP tracking under variable environmental conditions. In a typical fuzzy MPPT system, the input variables are the PV module's voltage and current, which are processed to evaluate the control output. Based on a predefined reference model, the fuzzy controller adjusts the duty cycle of the DC–DC converter to modulate the array's output impedance. This ensures that the operating point remains aligned with the MPP despite fluctuations in irradiance and temperature.

6.1. Fuzzification

The initial step in designing a fuzzy logic controller involves defining fuzzy sets for both input and output variables. This process requires a foundational understanding of the range and behavior of each variable involved in the system. Fuzzification serves as the interface between real-world input signals and the fuzzy inference engine, translating crisp numerical values into linguistic variables represented by fuzzy sets. These sets are characterized by membership functions, which describe the degree to which an input belongs to a particular fuzzy category. Membership functions are inherently system-dependent, with their shapes varying according to the nature and range of the variables they represent. In large-scale systems, configuring appropriate membership functions becomes a challenging and complex task, as it requires balancing precision, interpretability, and computational efficiency.

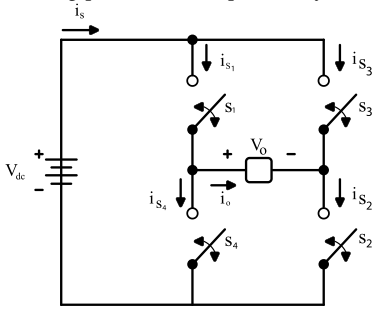

Figure 12: Equivalent circuit of a single-phase inverter.

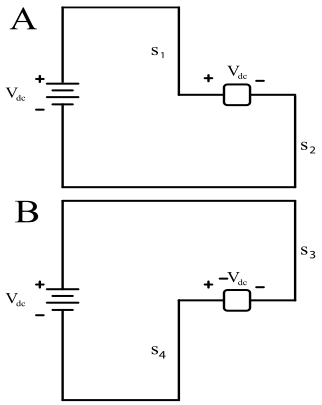

Figure 13. A: Connection state of switches S1, S2 B: Connection state of switches S3, S4.

6.2. Rules and deductions

During the inference stage of a fuzzy logic controller, a set of fuzzy rules is formulated to determine the control signal based on the input variables—typically the error and its derivative. Each fuzzy rule comprises two components: an antecedent (the 'if' part) and a consequent (the 'then' part). These rules represent expert knowledge or heuristic strategies and serve as the decision-making logic within the fuzzy inference system. By evaluating the degree to which input conditions satisfy each rule, the fuzzy controller generates an output that represents the required change in the control signal. This incremental output is then added to the previous control value at each sampling interval, effectively adjusting the system's behavior dynamically and adaptively.

6.3. Defuzzification

The output of the fuzzy controller is a fuzzy set, but a real quantity is required at the output. Therefore, the output of the fuzzy controller must be defuzzified.

The novel approach to fuzzy control involves the utilization of three inputs in lieu of two inputs, in conjunction with intelligent methods. In the phase controller, the inputs (E) are typically the power changes to the voltage changes and their changes (CE) in time t, which are expressed by the Equations (15) to (17). The output voltage of the module has also been utilized as the third input to enhance the output power of the PV module. It has been determined that the output of the phase controller is also a ΔD duty cycle.

$$E(t) = \frac{Ppv(t)-Ppv(t-1)}{Vpv(t)-Vpv(t-1)} \quad (15)$$

$$CE(t) = E(t) - E(t\text{-}1) \quad (16)$$

$$V_{pv}(t) \quad (17)$$

The structure of the fuzzy controller used to track the MPP is shown in Figure 14.

In this system, the Mamdani multiplication inference engine is used with a single fuzzifier as well as defuzzification of average centers and Gaussian membership functions, whose input and output relationship is as follows in Equation (18).

$$Y(X) = \frac{\sum_{L=1}^{M} \gamma^{L} \times [\prod_{i=1}^{n} \exp(-(\frac{Xi - Xi^{L}}{\sigma i}))]}{\sum_{L=1}^{M} [\prod_{i=1}^{n} \exp(\frac{Xi - Xi^{L}}{\sigma i}))]} \quad (18)$$

Y(X): Fuzzy system output
M: The number of fuzzy system rules
n: The number of input groups of the fuzzy system
γ^{L}: Centers of fuzzy system output groups
X_i^{L}: The centers of the input groups of the fuzzy system
σ_i: The degree of dispersion of the input groups of the fuzzy system.

In Equation (18), γ^{L}, X_i^{L}, and σ_i are factors that play a very important role in the accuracy of the fuzzy system. The more precisely these three parameters are adjusted in the fuzzy system, the better the fuzzy system performs. For this reason, we use particle swarm optimization (PSO) algorithms to adjust these three parameters.

The work process is such that the optimization algorithm determines the centers and sigmas of the fuzzy groups so that the cost function reaches its minimum value. The optimization process is done OFFLINE, and when the optimization algorithm determines the best centers and sigmas for the lowest cost function, it applies them to the fuzzy system, and after that, the fuzzy system consists of the centers and sigmas that the optimization algorithm has determined.

As illustrated in Figures 15 to 18, the fuzzy controller employs membership functions for its three input variables. The first input, typically representing the error (E), defined as the rate of change of power with respect to voltage, and the second input, its temporal derivative (CE), are each categorized into three linguistic labels: Negative (N), Zero (Z), and Positive (P). The third input, which corresponds to the module's output voltage, is also partitioned into the same three fuzzy sets (N, Z, P) to reflect its influence on the control process. The output variable of the fuzzy controller, which dictates the change in duty cycle (ΔD), is described by a broader range of linguistic terms, extending from Negative Very Large (NVL) to Positive Very Large (PVL), to capture fine variations in control action.The fuzzy rule base, as summarized in Table 1, is constructed based on the three input variables, each defined by three membership functions: N, Z, and P. Given that the fuzzy controller operates with three inputs and each input has three fuzzy sets, the total number of possible rule combinations is 33 = 2733 = 27.

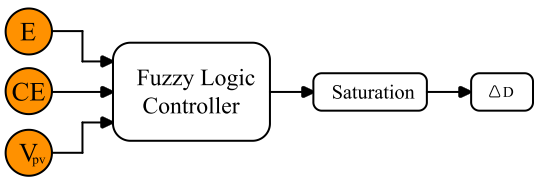

Figure 14. The adopted Fuzzy system.

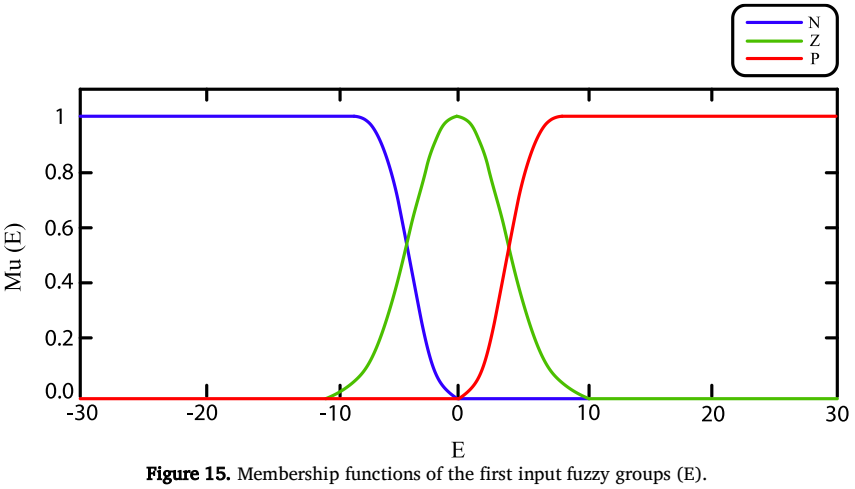

Figure 15. Membership functions of the first input fuzzy groups (E).

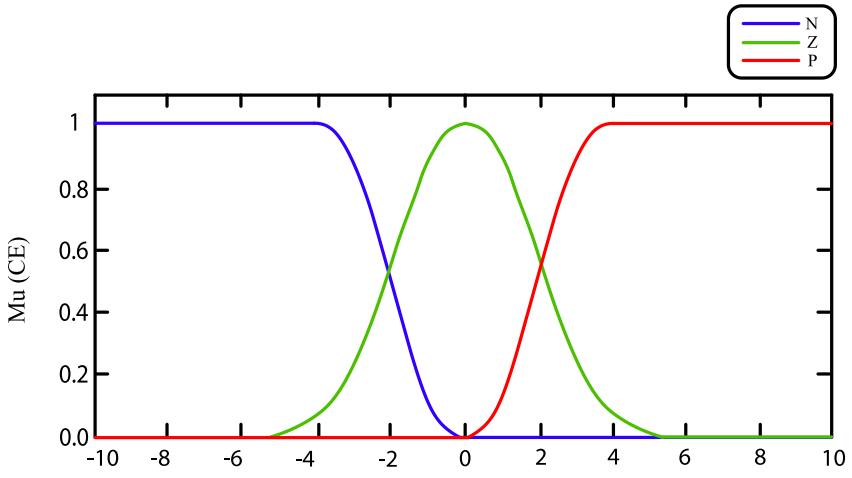

Figure 16. Membership functions of the second input fuzzy groups (CE).

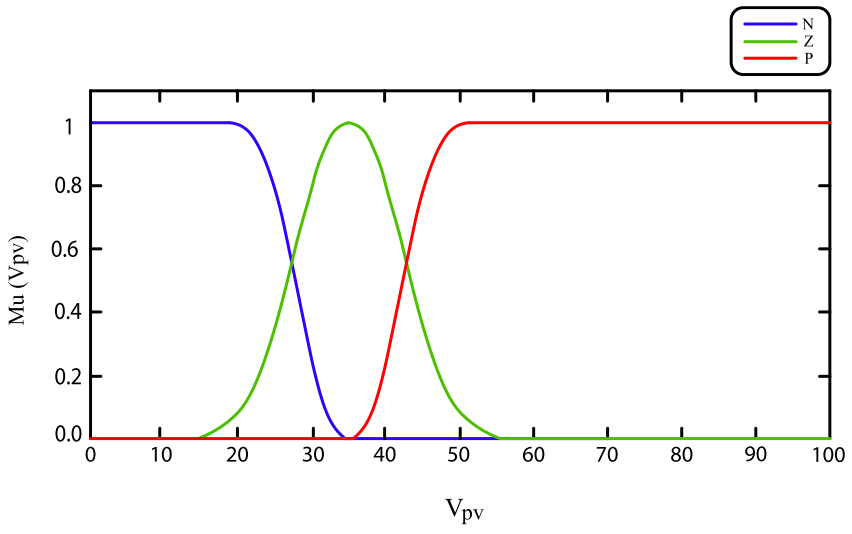

Figure 17. Membership functions of the third input fuzzy groups (Vpv).

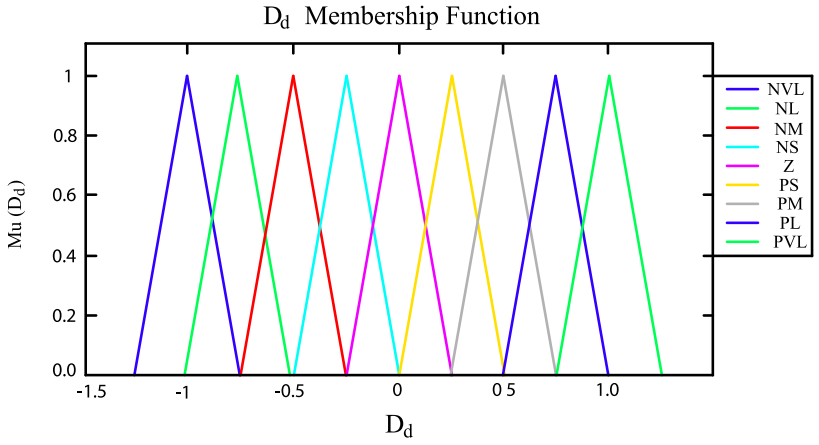

Figure 18. Membership functions of output fuzzy groups (ΔD).

Table 1. Fuzzy logic rules.

1.	Input 1	2.	Input 2	3.	Input 3	4.	Output
5.	N	6.	N	7.	N	8.	Z
9.	N	10.	N	11.	Z	12.	NS
13.	N	14.	N	15.	P	16.	NVL
17.	N	18.	Z	19.	N	20.	Z
21.	N	22.	Z	23.	Z	24.	NM
25.	N	26.	Z	27.	P	28.	NVL
29.	N	30.	P	31.	N	32.	PS
33.	N	34.	P	35.	Z	36.	Z
37.	N	38.	P	39.	P	40.	NS
41.	Z	42.	N	43.	N	44.	PS
45.	Z	46.	N	47.	Z	48.	NS
49.	Z	50.	N	51.	P	52.	NL
53.	Z	54.	Z	55.	N	56.	PM
57.	Z	58.	Z	59.	Z	60.	Z
61.	Z	62.	Z	63.	P	64.	NM
65.	Z	66.	P	67.	N	68.	PL
69.	Z	70.	P	71.	Z	72.	PS
73.	Z	74.	P	75.	P	76.	NS
77.	P	78.	N	79.	N	80.	PM
81.	P	82.	N	83.	Z	84.	Z
85.	P	86.	N	87.	P	88.	NM
89.	P	90.	Z	91.	N	92.	PM
93.	P	94.	Z	95.	Z	96.	PS
97.	P	98.	Z	99.	P	100.	Z
101.	P	102.	P	103.	N	104.	PVL
105.	P	106.	P	107.	Z	108.	PM
109.	P	110.	P	111.	P	112.	Z

These 27 fuzzy rules form the core of the decision-making mechanism, enabling the controller to generate appropriate adjustments to the duty cycle (ΔD) in response to changes in system behavior and environmental conditions.
Fuzzy controller parameters have been optimized to reduce power fluctuations around the MPP using the particle swarm algorithm. For optimization, it is necessary to choose the criterion or cost function as in Equation (19).

$$J = \frac{1}{N}\sum_{k=1}^{N}(Pref - P)^2 = 0 \quad (19)$$

npop**:** Number of particles
MAXit: Number of iterations
c_1, c_2: PSO parameters
W**:** Coefficient of inertia

The graph of the cost function will be shown in Figure 19. After optimization by PSO algorithm, membership functions of fuzzy controller are optimized as follows in Figure 20:

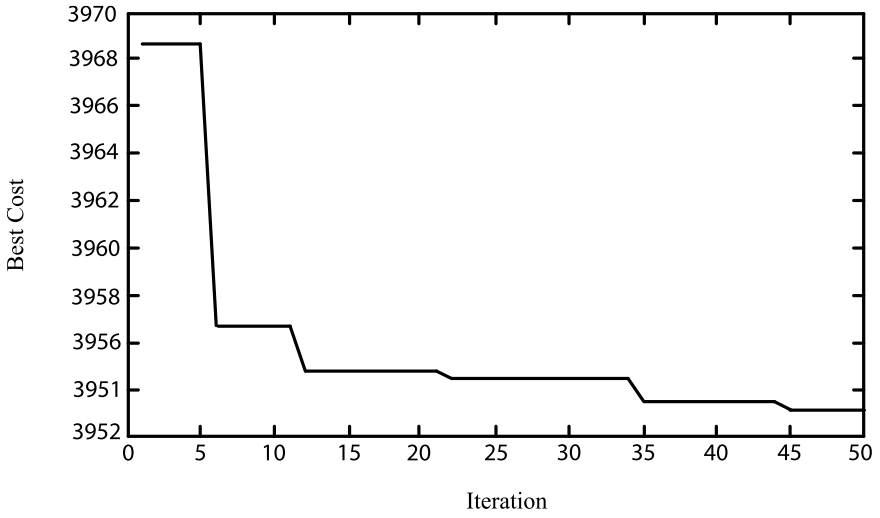

Figure 19. Cost function.

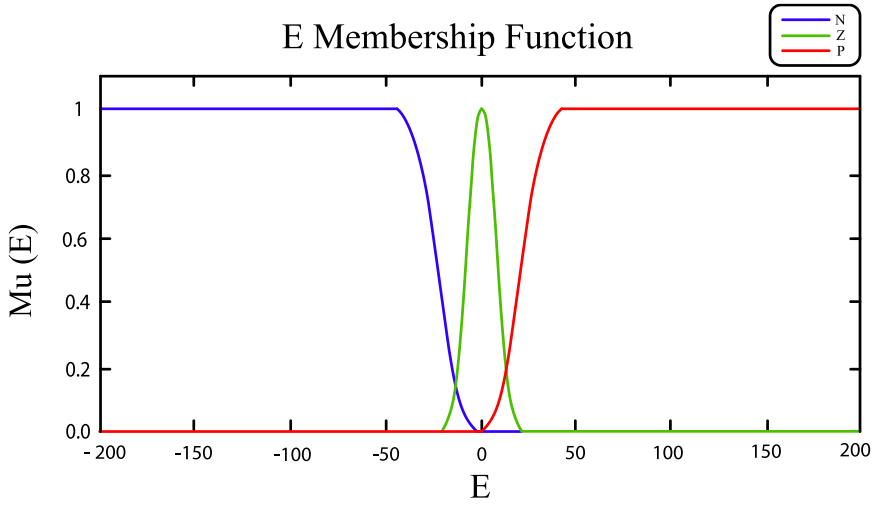

Figure 20. Membership functions of the first input fuzzy groups (E) after optimization.

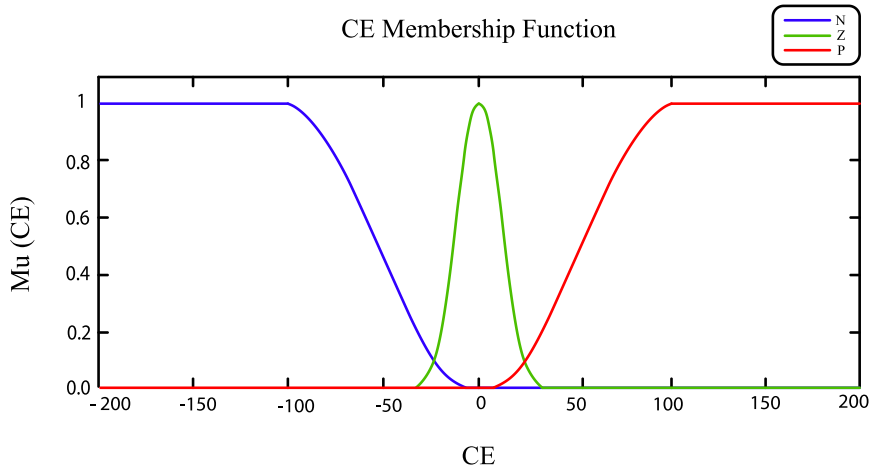

Figure 21. Membership functions of the second input fuzzy groups (CE) after optimization.

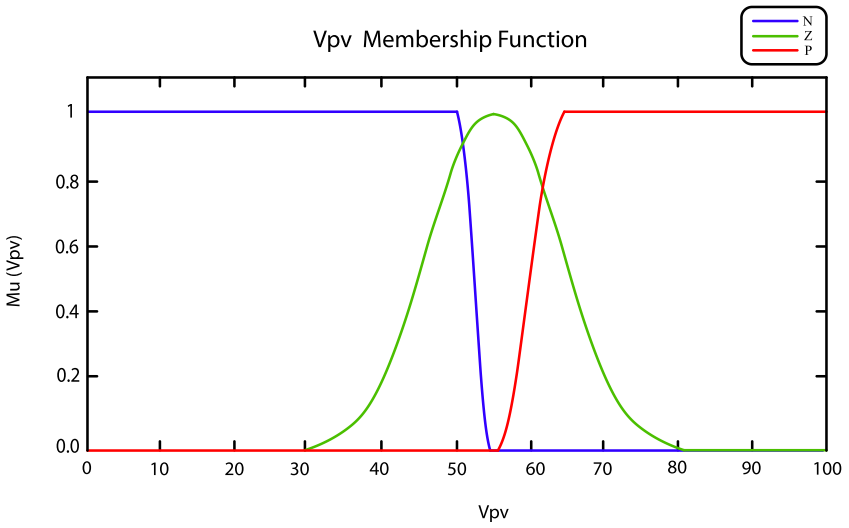

Figure 22. Membership functions of the third input fuzzy groups (Vpv) after optimization.

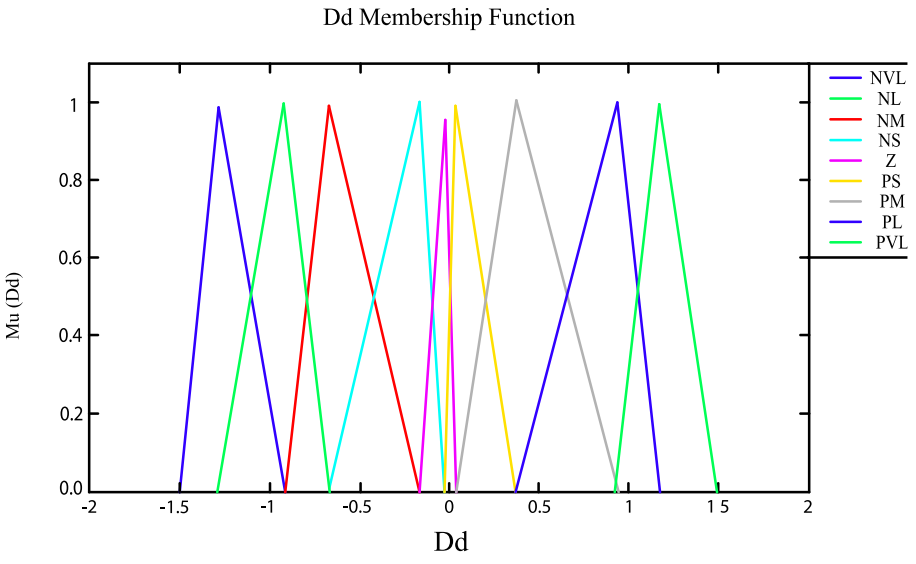

Figure 23. Membership functions of output fuzzy groups (ΔD) after optimization.

7. Simulation Results Utilizing MATLAB

"For simulation purposes in this study, the BP SX 150S PV module is selected. The simulation is implemented using MATLAB, where the PV module is modeled through a MATLAB Function Block. This block accepts two input parameters: solar irradiance (in kW/m^2) and cell operating temperature (in Celsius degrees), which is internally converted to Kelvin for accurate computation. These inputs are essential for dynamically replicating the behavior of the PV module under varying environmental conditions.

To evaluate the performance and efficiency of the proposed fuzzy logic control system, the simulation is first conducted on a standalone (grid-independent) PV system.

The MPPT algorithm is responsible for continuously tracking the optimal operating point to extract the maximum available power from the PV module. The actual regulation of PV operation at this point is achieved through a DC–DC converter, which adjusts its duty cycle based on the MPPT controller's output to ensure the module operates at or near the MPP.

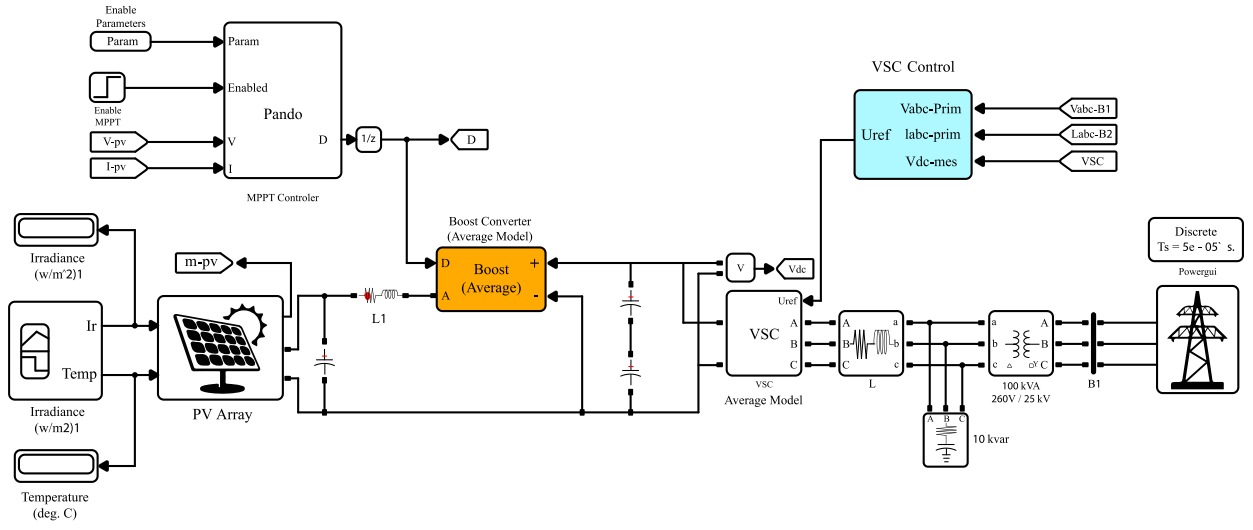

Figure 24. Grid-independent PV system.

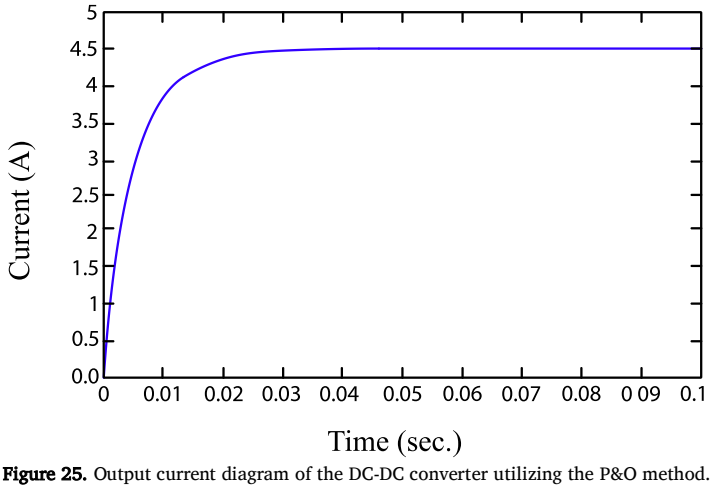

Figure 25. Output current diagram of the DC-DC converter utilizing the P&O method.

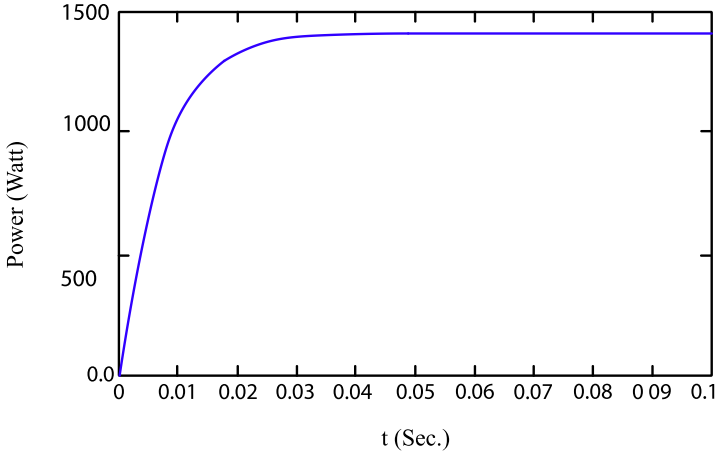

Figure 26. Output power diagram of the DC-DC converter utilizing the P&O method.

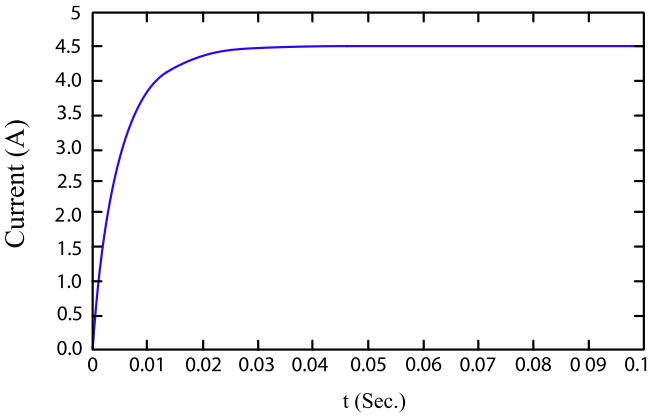

Figure 27. Output current diagram of the DC-DC converter utilizing fuzzy optimal control method.

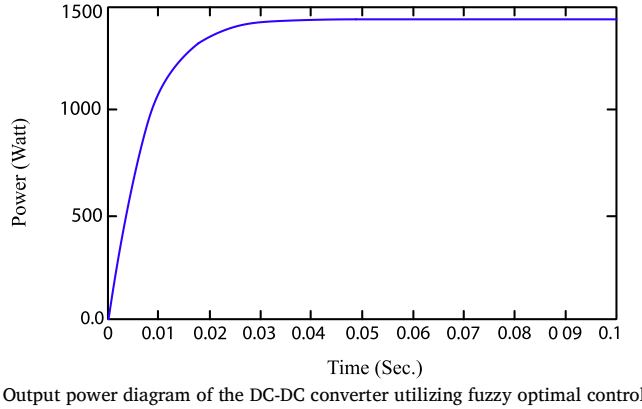

Figure 28. Output power diagram of the DC-DC converter utilizing fuzzy optimal control method.

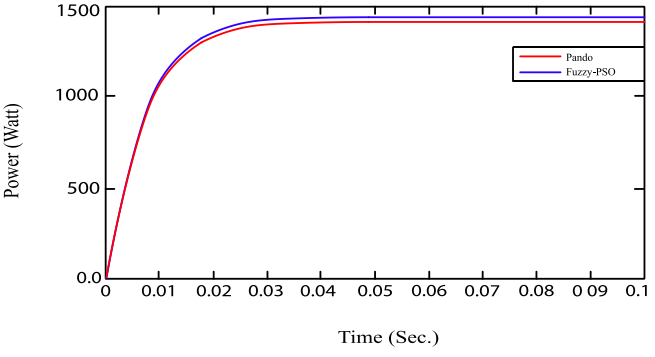

Figure 29. Comparison of tracked power by the optimal fuzzy method and the P&O method.

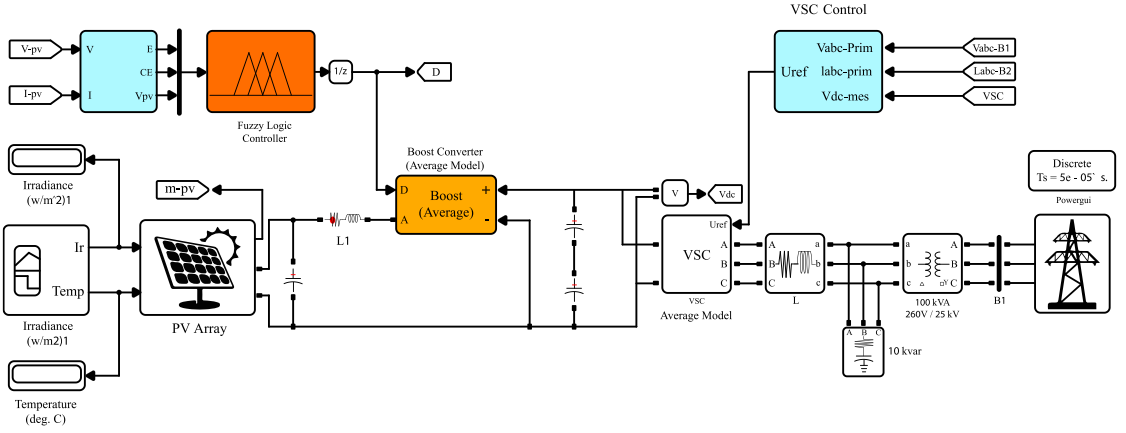

Figure 30. Grid-connected PV system with optimal fuzzy controller.

According to the results of the simulations, it is clear that the current and voltage ripple of the optimal phase control method is less than the P&O method, and also the power ripple will be less, and its better performance is proven. In the tracked power part, the optimal fuzzy control method has a higher value than the P&O method, which proves the proper performance of the proposed method.

In the following paragraphs, we simulate the designed PV system connected to the grid. First, the output power of the PV array is adjusted by the DC-DC converter, and then it is converted to alternating power by the direct power inverter. The single-phase voltage source inverter is used to connect to the low-voltage distribution network. The goal is to inject the maximum production power of the PV system into the grid. As a result, the injection current must be in phase with the network current. The network used includes a phase-locked loop (PLL) for synchronizing the power injected into the network, as well as an L-filter to reduce unwanted harmonics. A PLL is used to track the grid voltage even under severe harmonic conditions.

7.1. Network synchronization

One of the most important aspects of distributed production systems is synchronization with the network. The PV module and inverter must be able to adapt to the grid frequency and phase. The hysteresis current control method is used in this article.

7.2. Hysteresis current control method

In circumstances where the inverter is connected to the distribution network, the current control method is employed for synchronization.

At first, the network voltage is sent to the PLL to determine the frequency and phase of the network, and then, using the determined frequency and phase, we create the reference current. Then, the reference current is compared with the network current and determined by the hysteresis method and band determination. The inverter gates are switched. A PID controller is also used to control the range of the reference current. Multiply the coefficient obtained from the PID controller by the reference current so that the input voltage of the inverter does not exceed a desired value and is controlled.

7.3. PID controller

The Proportional–Integral–Derivative (PID) controller is a widely used feedback control mechanism that aims to minimize the error between a desired reference input and the system output. The effectiveness of a PID controller relies on the appropriate tuning of its three parameters: the proportional gain (Kp), the integral gain (Ki), and the derivative gain (Kd). These coefficients determine the controller's responsiveness, steady-state accuracy, and ability to predict system behavior, respectively.

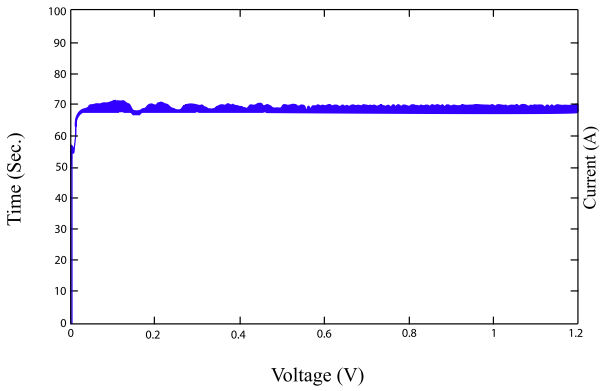

Figure 31. The output voltage of the PV module.

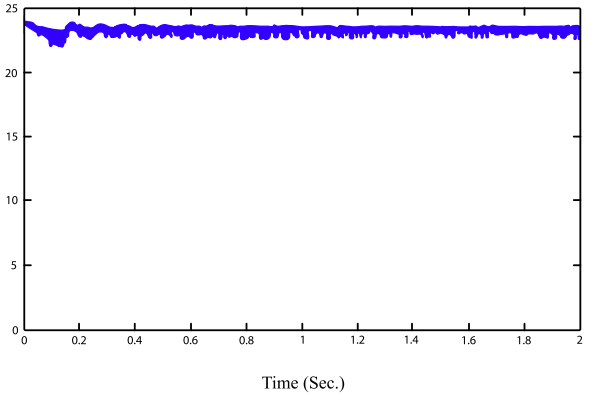

Figure 32. The output current of the PV module.

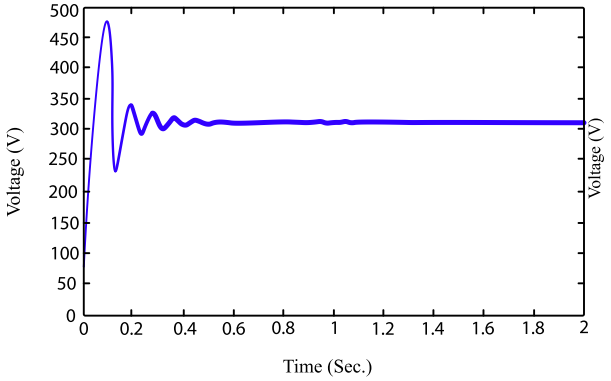

Figure 33. Boost converter output voltage.

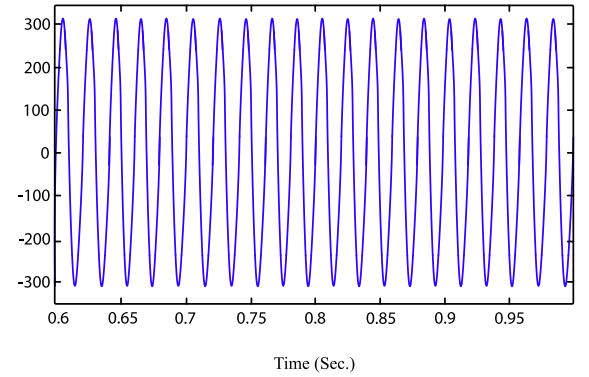

Figure 34. Network voltage.

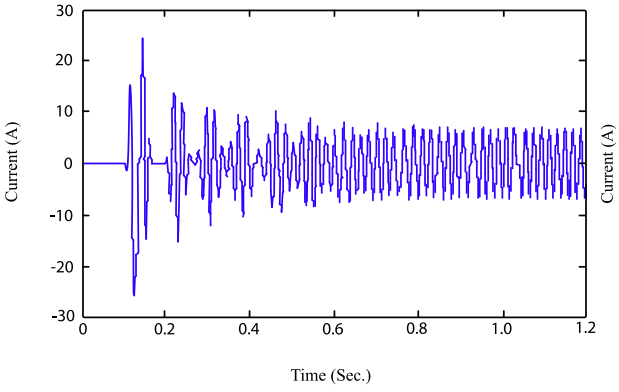

Figure 35. Reference current.

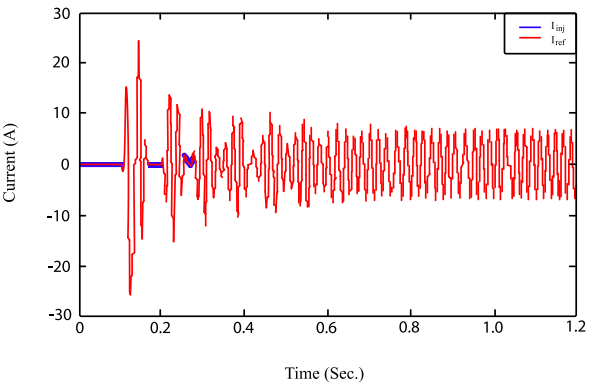

Figure 36. Reference current along with injected current to the grid.

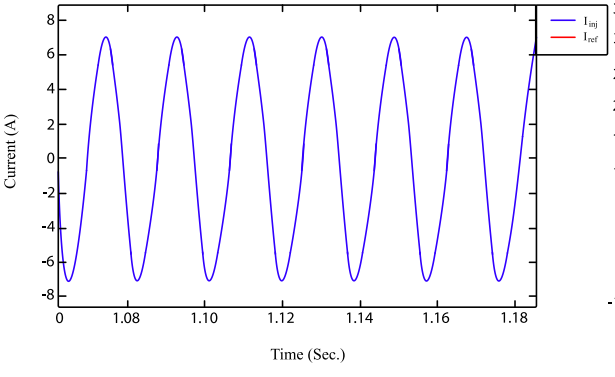

Figure 37. Reference current tracking by injecting current into the grid.

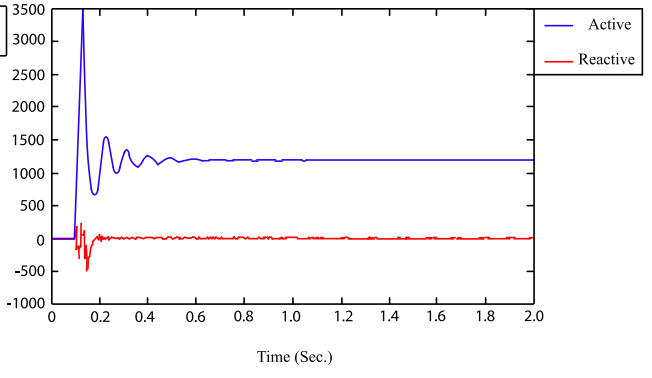

Figure 38. Active and reactive power injected into the network.

8. Conclusions

This study presented an intelligent, modified optimal fuzzy control strategy for MPPT in standalone PV systems. The objective was to minimize power fluctuations and enhance overall system efficiency. The proposed method was benchmarked against the conventional P&O technique, demonstrating superior performance in terms of tracking accuracy and stability. To further refine the controller's effectiveness, the PSO algorithm was employed to optimize the fuzzy controller's parameters, ensuring appropriate switching behavior. The optimized fuzzy controller significantly reduced ripple at the MPP and maintained stable operation under varying irradiance and temperature conditions. Additionally, the fuzzy-optimal control strategy was extended to a grid-connected PV system, successfully enabling maximum power transfer to the utility grid.

Abbreviations

K: Boltzmann's constant
I_{ph}: current generated from received photons
$I_{O.}$ Diode reverse saturation current
V: Voltage across the diode
Q: electrical charge
T: Junction temperature in Kelvin
N: Ideal diode coefficient (between 1 and 2)

References

[1] U.S. Energy Information Administration, *International Energy Outlook 2014*. Washington DC, 2014.
[2] L. D. Partian, *Solar Cells and Their Applications*. New York, NY, USA: John Wiley & Sons, 1995.
[3] M. R. Patel, and O. Beik, "Wind Power Systems," *Wind and Solar Power Systems*, pp. 37–62, 2021.
[4] International Energy Agency, *World Energy Outlook 2004*. Paris, France: IEA/OECD, 2004.
[5] M. Yaghoubi, "Studies of Environmental Compatible Buildings Using Domed Roof Architectures for Passive Cooling in Hot Arid Regions of Iran," *in Proceedings of Sustainable Energy Development in Asia Conference*, Beijing, China, Nov. 2008.
[6] M. S. Sivagamasundari, P. M. Mary, and V. K. Velvizhi, "Maximum Power Point Tracking for Photovoltaic System By Perturb And Observe Method Using Buck Boost Converter," *International Journal of Advanced Research in Electrical, Electronics and Instrumentation Engineering*, vol. 2, no. 6, pp. 2433–2439, 2013.
[7] K. Kobayashi, I. Takano, and Y. Sawada, "A Study of a Two Stage Maximum Power Point Tracking Control of a Photovoltaic System Under Partially Shaded Insolation Conditions," *Solar Energy Materials and Solar Cells*, vol. 90, no. 18-19, pp. 2975–2988, 2006.
[8] K. Irisawa, T. Saito, I. Takano, and Y. Sawada, "Maximum Power Point Tracking Control of Photovoltaic Generation System Under Non-Uniform Insolation by Means of Monitoring Cells," *Conference Record of the Twenty-Eighth IEEE Photovoltaic Specialists Conference - 2000 (Cat. No.00CH37036)*, pp. 1707–1710, n.d.
[9] T. Esram, J. Kimball, P. Krein, P. Chapman, and P. Midya, "Dynamic Maximum Power Point Tracking of Photovoltaic Arrays Using Ripple Correlation Control," *IEEE Transactions on Power Electronics*, vol. 21, no. 5, pp. 1282–1291, 2006.
[10] T. Noguchi, S. Togashi, and R. Nakamoto, "Short-Current Pulse Based Adaptive Maximum-Power-Point Tracking for Photovoltaic Power Generation System," *ISIE'2000. Proceedings of the 2000 IEEE International Symposium on Industrial Electronics (Cat. No.00TH8543)*, vol. 1, pp. 157–162.

[11] M. Masoum, H. Dehbonei, and E. Fuchs, "Theoretical and Experimental Analyses of Photovoltaic Systems with Voltage and Current-Based Maximum Power-Point Tracking," *IEEE Transactions on Energy Conversion*, vol. 17, no. 4, pp. 514–522, 2002.
[12] J. A. Jaleel, A. Nazar, and A. R. Omega, "Simulation on Maximum Power Point Tracking of the Photovoltaic Module Using LabVIEW," *International Journal of Advanced Research in Electrical, Electronics and Instrumentation Engineering*, vol. 1, no. 3, pp. 190–199, 2012.
[13] E. Jimenez-Brea, A. Salazar-Llinas, E. Ortiz-Rivera, and J. Gonzalez-Llorente, "A Maximum Power Point Tracker Implementation for Photovoltaic Cells Using Dynamic Optimal Voltage Tracking," *2010 Twenty-Fifth Annual IEEE Applied Power Electronics Conference and Exposition (APEC)*, pp. 2161–2165, 2010.
[14] C. Ben Salah, and M. Ouali, "Comparison of Fuzzy Logic and Neural Network in Maximum Power Point Tracker for PV Systems," *Electric Power Systems Research*, vol. 81, no. 1, pp. 43–50, 2011.
[15] B. N. Alajmi, K. H. Ahmed, S. J. Finney, and B. W. Williams, "Fuzzy-Logic-Control Approach of a Modified Hill-Climbing Method for Maximum Power Point in Microgrid Standalone Photovoltaic System," *IEEE Transactions on Power Electronics*, vol. 26, no. 4, pp. 1022–1030, 2011.
[16] R. Raja, L. U. Kumar, and S. R. Kumar, "Fuzzy logic controller for photovoltaic array simulator," 2013.
[17] S. Pirouzi, and A. Naderi, "Applying Sliding Mode Control Along with Particle Swarm Algorithm in Order to Optimally Control the System Wind Turbines with Variable Speed," *Journal of Green Energy Research and Innovation*, vol. 1, no. 2, pp. 64–80, 2024.
[18] BP SX051 – 051-watt multi crystalline photovoltaic module datasheet, 2001.
[19] B. Alatas, E. Akin, and A. B. Ozer, "Chaos Embedded Particle Swarm Optimization Algorithms," *Chaos, Solitons & Fractals*, vol. 40, no. 4, pp. 1715–1734, 2009.
[20] R. Poli, J. Kennedy, and T. Blackwell, "Particle Swarm Optimization," *Swarm Intelligence*, vol. 1, no. 1, pp. 33–57, 2007.
[21] M. A. Mahmud, H. R. Pota, and M. J. Hossain, "Nonlinear Current Control Scheme for a Single-Phase Grid-Connected Photovoltaic System," *IEEE Transactions on Sustainable Energy*, vol. 5, no. 1, pp. 218–227, 2014.
[22] Anonymous, "Power Electronics Converters Processing AC Voltage and Power Blocks Geometry," *ADVANCED POWER ELECTRONICS CONVERTERS*, pp. 56–87, 2014.
[23] S. E. Aminoroayaye yamani, M. Bahramian, and A. A. Ghadimi, "Improving Low Voltage Ride-Through Capability of Doubly-Fed Induction Generator Wind Farms Using Superconducting Fault Current Limiter," *Journal of Green Energy Research and Innovation*, vol. 1, no. 2, pp. 15–30, 2024.
[24] M. Mohseni, A. Niknam Kumleh, M. Alibakhshi, and M. Sheikhi Abou Masoudi, "Improving the Maximum Power Point Tracking in a Photovoltaic System Based on the Resistance-Predictive Method," *Journal of Green Energy Research and Innovation*, vol. 1, no. 2, pp. 81–102, 2024.

Declaration of competing interest

The authors declare that they have no known competing financial interests or personal relationships that could have appeared to influence the work reported in this paper. The ethical issues, including plagiarism, informed consent, misconduct, data fabrication and/or falsification, double publication and/or submission, redundancy, have been completely observed by the authors.

Bibliography

Asaad Shemshadi was born on Nov 1, 1979. He received the B.Sc. degree from the Shiraz University, in 2003, the M.Sc. degree from the Kashan University, Iran in 2007, and PhD degree from Khaje Nasir Toosi University of Technology in 2014, all in Electrical engineering. His research interests are: Vacuum Interrupters design and analysis, high voltage simulations, thermal plasma modeling, high voltage equipments design, transients in vacuum arc quenching, renewable energies and pulsed power.
Email: shemshadi@arakut.ac.ir
ORCID: 0000-0002-7271-9933
Contribution Statement: Conceptualization, Data curation, Formal analysis, , Validation, Roles/Writing - original draft, Writing-review & editing.

Hamidreza Haghighi was born on October 2, 1999 in Esfahan, Iran. He received his B.Sc and MSc. degrees from Arak University of Technology, in the field of electrical engineering. His Interests are: power systems transients, Electricity market, power system dynamics and renewable energies.
Email: k-khandani@araku.ac.ir
ORCID: 0009-0004-1737-5666
Contribution Statement: Formal analysis, Investigation, Software, Roles/Writing-original draft, Writing-review & editing.